

Characterization and properties of an advanced composite substrate for YBCO-coated conductors

Mangmang Gao^a, Hongli Suo^{a,*}, Yue Zhao^a, J.-C. Grivel^b, Yanling Cheng^a, Lin Ma^a, Rong Wang^a, Peikuo Gao^a, Jianhong Wang^a, Min Liu^a, Yuan Ji^c, Shengzhong Kou^d

^a Key Laboratory of Advanced Functional Materials, Ministry of Education, College of Materials Science and Engineering, Beijing University of Technology, 100 Pingleyuan, Chaoyang District, Beijing 100022, China

^b Materials Research Department, Risø National Laboratory, Technical University of Denmark, Frederiksborgvej 399, DK-4000 Roskilde, Denmark

^c Institute of Microstructure and Property of Advanced Materials, Beijing University of Technology, 100 Pingleyuan, Chaoyang District, Beijing 100022, China

^d State Key Laboratory of GanSu Advanced Non-ferrous Metal Materials, Lanzhou University of Technology, Lanzhou 730050, China

Received 13 April 2009; received in revised form 22 August 2009; accepted 21 October 2009

Available online 22 November 2009

Abstract

Thin, biaxially textured Ni5W/Ni12W/Ni5W composite substrates for coated conductor applications have been fabricated. The particularity of this three-layer composite configuration resides in the elemental diffusion between the outer layer and the core layer. Due to the migration of elemental W, the diffusion layer in the as-annealed substrate becomes broader than that of the as-rolled substrate. The obtained tape has a sharp cubic texture on the Ni5W outer layers, and the volume fraction of cubic grains exceeds 98.8% ($<10^\circ$) at the outer surfaces. In situ electron backscatter diffraction strain–stress analysis shows that the high-quality cubic texture was stable until elongations as high as 2%. The yield strength of the composite substrate approaches 240 MPa and its saturation magnetization at 77 K has been strongly reduced with respect to pure Ni and Ni5W substrates. The present results demonstrate that this advanced three-layer substrate is suitable for the epitaxial growth of the LZO buffer layers.

© 2009 Acta Materialia Inc. Published by Elsevier Ltd. All rights reserved.

Keywords: Composite substrate; Coated conductors; Cubic texture; In situ EBSD tensile test; Texture stability

1. Introduction

The Rolling Assisted Biaxially Textured Substrate (RABiTS™) method for Ni and Ni-based alloys developed at Oak Ridge National Laboratory, USA is one of the most promising approaches for economic large-scale production of high-temperature superconducting (HTS) $\text{YBa}_2\text{Cu}_3\text{O}_{7-\delta}$ (YBCO) tapes carrying large currents at 77 K in the presence of magnetic fields. In the RABiTS route, the textured substrate plays an important role, supplying the necessary strength to the tape and constituting a

basis for epitaxial growth of the buffer layer and the conductor layer [1,2]. Among various metallic combinations, Ni–W alloys have been systematically investigated and widely used as a substrate material for coated conductors during the past decade [3–6]. Until now, although 100 m lengths of Ni–5 at.% W tape with cube texture and high surface quality have been produced by a number of groups or companies [7–10], the mechanical and magnetic behaviors of the substrates can still be improved by increasing the tungsten content in the Ni–W alloy. The sharp cube recrystallization texture cannot be easily formed in high-tungsten ($\text{W} > 7$ at.%) NiW alloys by means of cold rolling and recrystallization annealing, due to the reduction of stacking fault energy (SFE) originating from the increased

* Corresponding author. Tel.: +86 10 67392947.
E-mail address: honglisuo@bjut.edu.cn (H. Suo).

strength and possibly from the presence of short-range order in these alloys [11,12]. This problem has been solved by the design of so-called composite substrates [13–15]. The composite substrate has a sandwich architecture, where the outer layers are based on low-W Ni–W alloy facilitating the formation of a sharp cubic texture, with high-W Ni alloy at the core layer ensuring both mechanical reinforcement and lower magnetization of the whole substrate.

Previously, we have successfully fabricated these new composite substrates with a sharp cubic texture and reduced saturation magnetization from a multilayer ingot which was synthesized by the sparking plasma sintering (SPS) technique and powder metallurgy (PM). The techniques for fabricating a series of composite tapes with both sharp cubic texture and enhanced strength such as Ni5W/Ni9W/Ni5W and Ni5W/Ni12W/Ni5W have been reported [16–18]. In this paper, a Ni5W/Ni12W/Ni5W composite tape with a similar thickness of the three layers has been investigated in depth. Various performances are reported, including the macro- and microtexture, and the tensile effect on the orientation measured by in situ electron backscatter diffraction (EBSD). The successful deposition of a high-quality La₂Zr₂O₇ (LZO) buffer layer directly on this composite substrate has also shown that the present composite substrate is appropriate for further developments of coated conductor tapes.

2. Materials and methods

2.1. Preparation of composite substrate

The Ni powders (99.9%) and W powders (99.8%) from Beijing MENGTAI Technology Development Center were mixed by ball milling (Fritsch P6) in argon atmosphere with alloy compositions of Ni–5 at.% W (Ni5W) and Ni–12 at.% W (Ni12W), respectively. The mixed powders were first packed into a graphite mold in the sequence Ni5W/Ni12W/Ni5W and then cold pressed under an axial pressure of 15 MPa. The SPS technique under a pressure of 30 MPa was employed to synthesize the starting composite ingot at a temperature of 800 °C. The sintered composite ingot was then cold rolled to 80 μm thickness, with reduction ratios of below 5% per pass, the total reduction being larger than 99%. The rolled composite metallic tapes were heat treated by a two-step annealing process, holding the sample at a lower temperature (about the recrystallization temperature) for half an hour before reaching the annealing temperature of 1250 °C in a flowing Ar–4% H₂ atmosphere in order to obtain the desired orientation at the top surface of the composite substrate.

2.2. Microstructure and elemental distribution measurement

The microstructure of the composite substrate was observed by scanning electron microscopy (SEM; JEOL JSM 6500F). Energy-dispersive X-ray analysis (EDAX) was employed to analyze both the elemental content and

distribution through the cross-section of the cold-rolled composite and the annealed composite tape.

2.3. Texture analysis

The macro-texture of the recrystallized composite tape was characterized by means of a Bruker D8 X-ray diffractometer using Cu K_α radiation. For further analysis, microtexture and misorientation distribution information on the composite tapes was acquired by the collecting data by means of electron backscattering diffraction (EBSD; TSL) (on a 600 μm × 400 μm area). The cubic texture component was evaluated using orientation imaging microscopy (OIM) software. Additionally, the microstructure analysis with in situ tension was characterized on the surface of the composite substrate using SEM comprising EBSD analysis and an in situ tensile system. The samples size was 15 mm × 3 mm × 75 μm.

2.4. Mechanical and magnetic properties

The stress–strain curves were determined by the tensile tester attached to the EBSD system with tapes 15 mm long and 3 mm wide, at a speed of 0.4 mm min^{−1}. The loading direction was along the [1 0 0] crystallographic direction of the annealed substrates. A Quantum Design (PPMS9) magnetometer was used to measure the *M*–*H* hysteresis loops at 77 K in order to examine the magnetization of the as-fabricated composite tapes.

2.5. Growth of LZO buffer layer on Ni5W/Ni12W/Ni5W composite substrate

The 5 mm × 5 mm composite substrates were cleaned by methanol and acetone in an ultrasonic bath for 20 min before coating. Spin coating was used to deposit the precursor films at a speed of 3000 rps for 60 s. Subsequently, the coated precursor films were annealed at 1150 °C for 15 min in a continuous reduced gas flow of mixed Ar–4% H₂ in order to protect the substrate from oxidation. After heat treatment, the samples were quenched to room temperature. The texture of the LZO films were characterized by X-ray diffraction (XRD) (*θ*/*2θ*-scan, *ω*-scan and *φ*-scan).

3. Results and discussion

3.1. Cross-section of the composite substrate

Fig. 1a shows a SEM backscattering cross-sectional image of the as-rolled Ni5W/Ni12W/Ni5W multilayer tape with a thickness about 75 μm including both Ni5W outer layers of about 25 and 20 μm thickness, respectively, and the 30 μm thick Ni12W core layer after 99% total deformation. The relative thickness of the three layers has changed with respect to the original thickness of the starting ingot, due to the different plastic deformation of the outer and

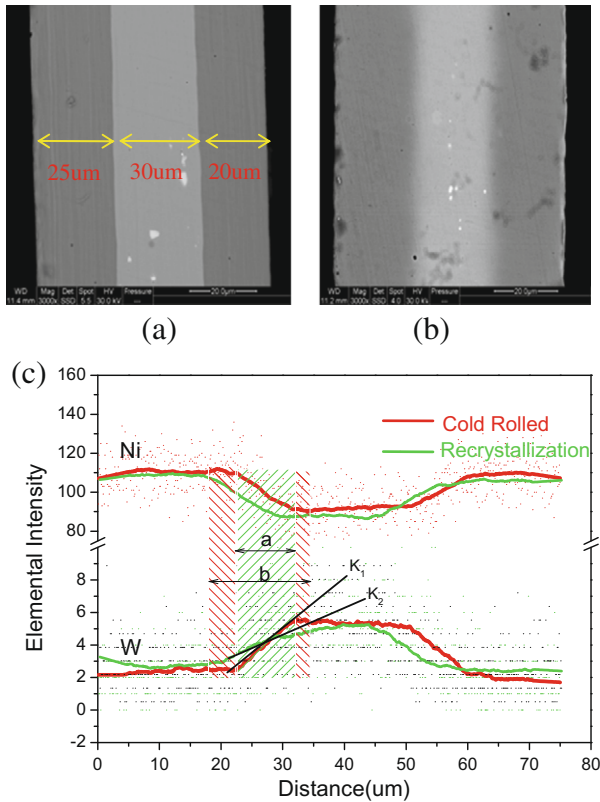


Fig. 1. SEM backscattering diffraction of: (a) as-rolled 75 μm thick Ni5W/Ni12W/Ni5W composite substrate; (b) as-annealed 75 μm thick Ni5W/Ni12W/Ni5W composite substrate; (c) Ni and W elemental distributions along the cross-section of both as-rolled and as-annealed composite substrates as determined by EDAX.

inner layers during the deformation process. The thickness difference of the two Ni5W outer layers of the cold-deformed tape is caused by the preparation stage, during which the starting ingot has been submitted to a mechanical polishing in order to remove the oxidation layer formed during the SPS process. It was observed that this tri-layer assembly did not delaminate after heavy rolling, in spite of the large difference in strength between the outer and inner layers. The good connectivity and clear boundary between Ni5W outer layer and Ni12W core layer are demonstrated in Fig. 1a. The key point of the design is to press the three powder layers together and to sinter them as a gradient composite to achieve chemical connectivity. Fig. 1b shows the SEM backscattering image of the as-annealed composite tape, the interlayer boundary being smeared out due to the elemental diffusion during the high-temperature processing. Thus, the diffusion layer of the as-annealed tape is broader than that of the as-rolled composite tape.

Fig. 1c shows the Ni and W distribution along the cross-section of the as-rolled composite tape (red line)¹ and the as-annealed tape (green line) measured by EDAX line

scanning. A continuous gradient of Ni and W was found at the interface between the outer and inner layers. At the same time, the elemental gradient diffusion layers could also be observed in both as-rolled and as-annealed composite tapes, which is in good agreement with the diffusion connectivity type of the starting ingot. Moreover, in comparison with the as-rolled composite tape, the boundary of the diffusion layer grew towards the inner core after annealing treatment. In other words, W migrated from the core to the outer layer, which is the cause for a more diffused interface width (Fig. 1b) in the as-annealed tape with respect to the as-rolled tape. It can be also verified that the slope of the W distribution line (K_2) in the diffusion area of the as-annealed tape is smaller than the value (K_1) of the as-rolled composite tape, thus indicating that the elemental gradient in the diffusion layer of the as-annealed tape is lower than that of the as-rolled tape. Consequently, the W elemental content at the surface area of the as-annealed tape is slightly higher than that of the as-rolled tape because of the W migration from the inner to the outer layer (correspondingly, the Ni elemental content in the surface area of as-annealed tape is lower than that of the as-rolled tape).

3.2. Macro-texture characterization of the Ni5W outer layer of the composite tape

X-ray detection was used to determine the macroscopic texture of the composite substrate. Fig. 2 shows the (1 1 1) and (2 0 0) pole figures of the outer Ni5W layer for the recrystallized tape. Clearly, four sharp peaks are present in the (1 1 1) pole figure and the intensities are concentrated on the four symmetrical positions, indicating that a pure and sharp (0 0 1) $\langle 100 \rangle$ cubic texture was obtained on the Ni5W surface layer of the Ni5W/Ni12W/Ni5W tape after recrystallization at 1150 $^{\circ}\text{C}$ for 60 min. Similarly, the (2 0 0) pole figure also shows a good out-of-plane orientation in the Ni5W layer of the recrystallized composite tape.

Fig. 3 shows the ODF section (φ_2 from 0 $^{\circ}$ to 90 $^{\circ}$) for the recrystallized samples. A sharp cubic texture was observed in the surface layer, which is consistent with our observation from pole figures. The maximum ODF value of the cube texture component is equal to 122.7 in this tape, indi-

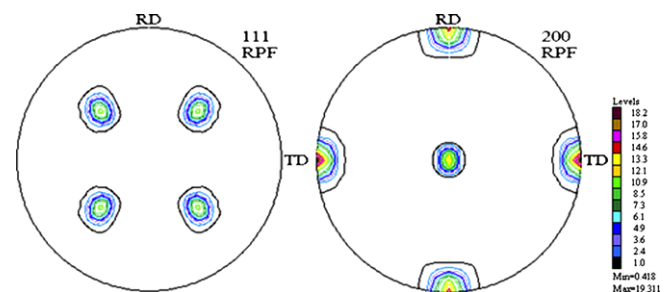


Fig. 2. X-ray (1 1 1) and (2 0 0) pole figures of the Ni5W layer of as-annealed composite tapes.

¹ For interpretation of color in the text, the reader is referred to the web version of this article.

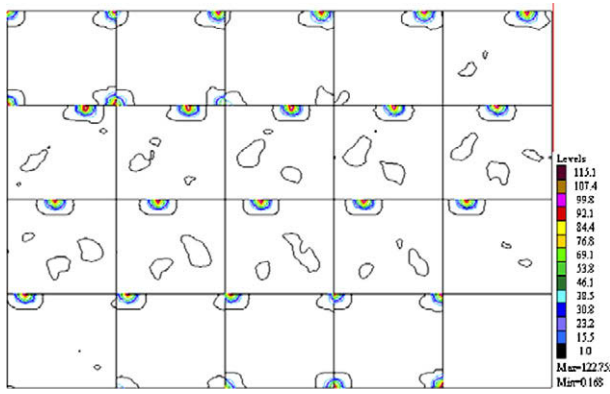


Fig. 3. Cross-section of the orientation distribution function (ODF) for the Ni5W layer of composite tape.

the outer layer, which increased the W content of the outer layer. It is well known that the cube texture is not easily obtained in NiW alloys with high W content because of the reduced SFE [19]. The present results show that the diffusion of the W element did not affect the formation of the cube texture of this composite tape after annealing.

3.3. Local microtexture characterization of the Ni5W outer layer of the composite tape

In order to evaluate the local texture, EBSD was employed to analyze the Ni5W surface layer of the annealed samples. Fig. 4a shows the EBSD color-coded image of neighbor grains with (0 0 1) <100> cube texture within a misorientation angle of 10° in the Ni5W surface layer in a composite tape measured in a randomly chosen area of 600 μm × 400 μm. The percentage of the grains with (0 0 1) <100> cubic orientation exceeds 98.8%, indicating that a

cating that a high-quality of cube texture was formed after recrystallization, although the W has been diffusing toward

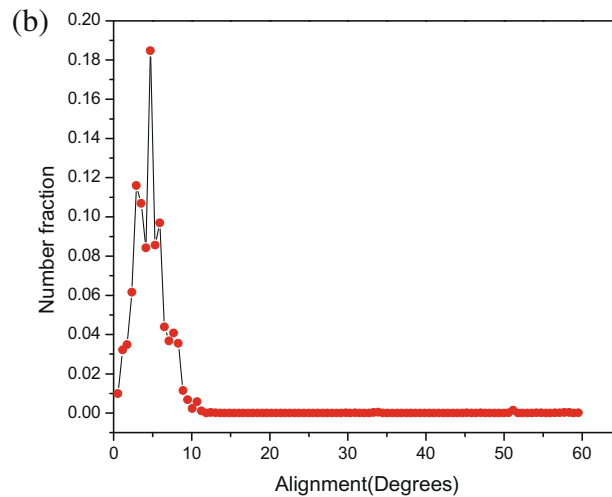
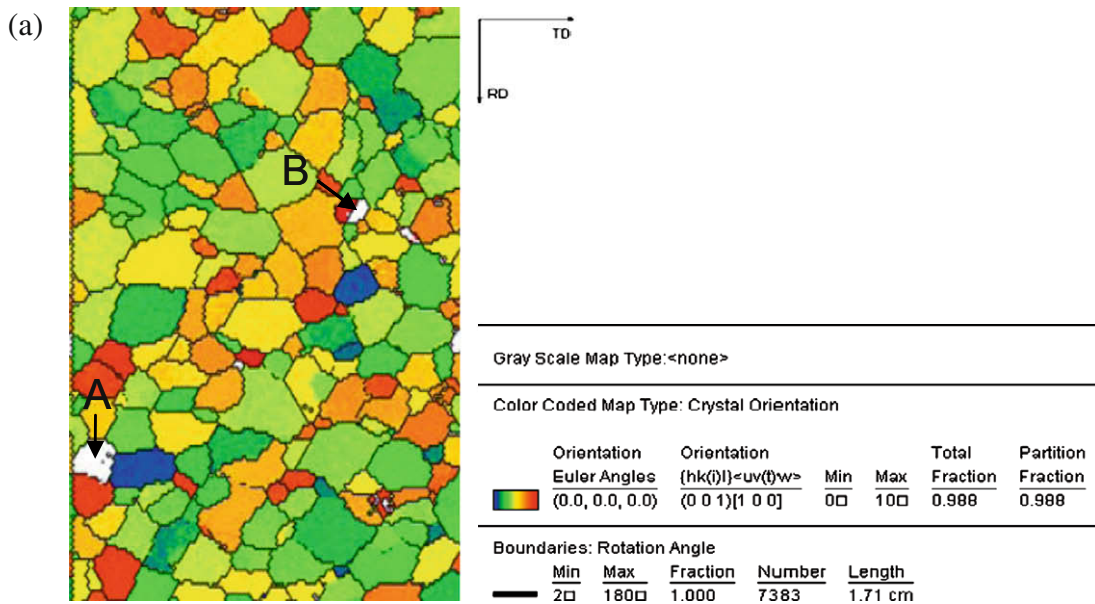


Fig. 4. EBSD data: (a) map of the misorientation distribution of the recrystallized composite tape and (b) number fraction of the misorientation distribution.

sharp cube texture has been formed. This result is also in good agreement with the result of X-ray analysis. Meanwhile, off-cube grains can be seen in the map (the white grain in Fig. 4a). It includes the two main types of off-cube grains: an equiaxial grain type (grain A) and a twin grain type (grain B). According to our previous work, the equiaxial grains can be avoided by means of a modification of the annealing process. After optimization of the procedure, a sharp cube texture can be obtained by both optimizing the annealing temperature and prolonging the annealing time. Fig. 4b is a plot of the number fraction of the cubic grains with misorientation angle on the outer Ni5W surface in an annealed composite substrate calculated by OIM. The number fraction of cubic grains within a misorientation angle of 6° exceeds 81% and a peak appears at 5° . This result shows a high-quality of cube texture and further confirms that the outer Ni5W layer in annealed substrate has a sharp cube texture which is equivalent to that of the single-layer Ni5W substrate.

3.4. In situ EBSD analysis of the microtexture of a Ni5W surface layer of the composite tape during tensile tests

The substrates are submitted to a certain strain during further coated conductor processing: growth of a buffer layer and the YBCO layer on its surface in a reel-to-reel process, at temperatures ranging between 800 and 1100 °C. It is thus necessary to investigate the stability of the microtexture of the outer Ni5W layer in the composite tape under tensile stress and at high-temperature to avoid the degradation of the cubic texture, which may subsequently affect the quality of the epitaxial layers. It was reported [20] that the substrate does not withstand strains above 0.5% in compression and 0.2% in tension; and the stress at low strain (e.g. 0.2% yield strength) is more critical for the substrate material in many applications. In this work, we have investigated the in situ microtexture of the Ni5W layer of the composite tape under tensile conditions.

The stress–strain data of the Ni5W/Ni12W/Ni5W composite tape are plotted in Fig. 5. The sample was fixed in

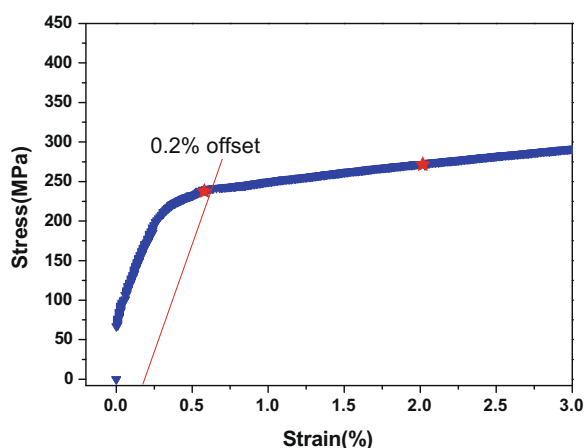


Fig. 5. The stress–strain curve of the Ni5W/Ni12W/Ni5W composite tape measured by tensile testing coupled with in situ EBSD analysis.

Table 1

The cube texture contents in the Ni5W outer layer of the composite substrate under the various strain states.

	$\varepsilon = 0\%$	$\varepsilon = 0.5\%$	$\varepsilon = 2\%$
Cube texture content	98.8	99	98.7

the tensile tester that was attached to the EBSD system, giving the possibility of analyzing the evolution of the surface misorientation of the outer Ni5W layer in situ during processing under tensile conditions. The sample was pulled along the rolling direction at a speed of 0.4 mm min^{-1} . Meanwhile the EBSD data were recorded at several strain stages (the original stage, the elongation percentages corresponding to 0.5% and 2% stages) in order to evaluate the microtexture of the outer Ni5W layer in the composite substrate under tensile processing conditions. From the strain–stress curve, it was found that the yield strength ($\delta_{0.2}$) of the composite substrate exceeds 240 MPa. This value is satisfied to the required value of 200–250 MPa for practical applications of coated tapes predicted by Goyal et al. [21].

As shown in Table 1, the percentage of the cube grains is almost unchanged after elongation, and the amount of cube texture within the misorientation angle of 10° are 99.8%, 99% and 98.7% at the original stage and at 0.5% and 2% elongations, respectively. These results indicate that the cube texture at the Ni5W layer surface of the as-obtained composite substrate can sustain a certain stress–strain. In particular, when the elongation percentage reaches 0.5%, which corresponds to the application limit of the coated tapes, the cube texture is still stable. Furthermore, the sharp cube texture present on the Ni5W outer layer when the elongation rate is as high as 2%, is markedly higher than the practical application condition for coated conductors. This result shows that Ni5W/Ni12W/Ni5W composite substrates, having a stable and high-quality cube texture, can be used for epitaxial growth of the buffer layer and YBCO film using a reel-to-reel technology, where a tension is applied to the substrate during processing.

Although the percentage of the cubic grains of the Ni5W surface layer was not markedly decreased during the tension process, some of the grains have been rotated by a small angle relative to the cube grains. Fig. 6a shows the EBSD mappings recorded on the same area of the Ni5W surface layer after different elongation stages, i.e. 0%, 0.5% and 2%, respectively. It can be seen that the colors of individual grains have changed slightly with increasing strain values, which illustrates that the strains along the rolling direction are the origin of the grain misalignment relative to the standard (0 0 1) $\langle 100 \rangle$ cube texture. From Fig. 6a, some grains within misorientation angles about 10° (those grains with (0 0 1) $\langle 100 \rangle$ orientation within misorientation angles about 10° were defined to be cube textured) can be observed. Due to the tension effect, some grains are changed from cubic-oriented (within a misorientation angle of 10°) into off-cubic grains, or conversely changed from off-cubic grains into cube-oriented grains.

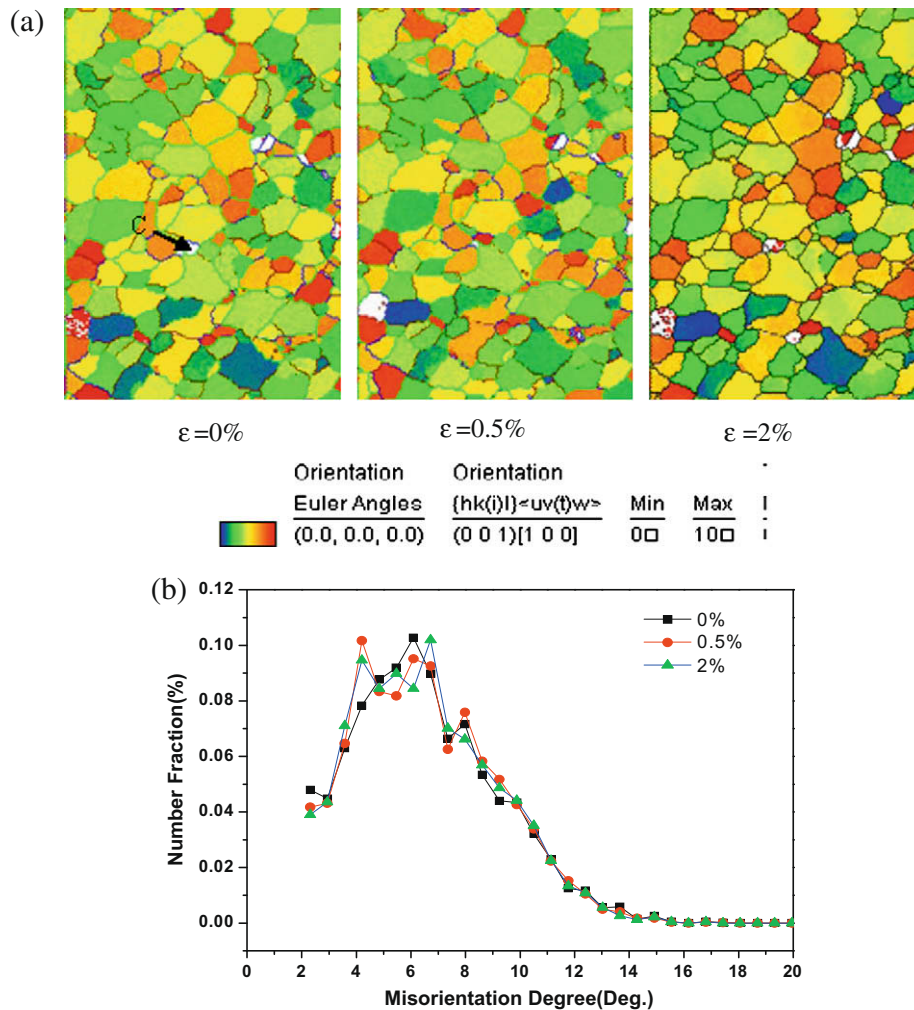


Fig. 6. (a) EBSD images and (b) the number fractions of small-angle grains at the surface of the Ni5W layer submitted to various tensile stresses.

Thus, the total percentage of cubic grains is unchanged. The trend of misorientation angle change is not simply related to the increase in elongation. For example, the grain C, an off-cubic grain at 0% elongation stage, is transformed into a cubic grain when the elongation reaches 0.5%. The decrease in the misorientation angle resulted from the grains slipping along the $\langle 111 \rangle$ crystal plane, but it is transformed to an off-cubic grain again when the elongation percentage increased to 2%. This is possibly caused by the varieties of slipping mechanisms in the deformation processing. The slipping mechanism needs further work for complete understanding.

Fig. 6b shows the number fractions of the small-angle grains of the Ni5W surface layer for various tensile strains. It was observed that the misorientation angles were mainly changed in the range of 4–8° for the three tension stages. The misorientation angle of the cubic grains was preferentially concentrated around 7° in the 0% elongation state of the composite substrate, and was changed to 4° for the elongation rate of 0.5%, indicating that all the cubic grains are more concentrated on the $(001)\langle 100 \rangle$ cube orientation. The maximum value of the number fraction of the

cubic grains appeared at 7° for 2% elongation, indicating that the quality of the cubic grains drops slightly compared to that of the 0.5% tension stage. Nevertheless, the quality of texture on the outer Ni5W layer is still high enough to allow further deposition of buffer and conductor layers, even for elongations reaching 2%.

Since the critical current density (J_c of the YBCO conductor layer) is strongly dependent on the grain boundary angle, it is also necessary to characterize the grain boundaries of the composite tapes at different strain stages. Fig. 7a shows the grain boundary distribution maps of the outer Ni5W layers for various elongations. The length of grain boundaries with low misorientation angles reaches 87.2%, 88.3% and 88.4%, respectively, at different elongation stages, indicating that the grain boundaries are very stable. In spite of such large elongations, the grain boundaries are divided into several fragments due to the various misorientation angles. Fig. 7b shows the length fractions for misorientation angles of 2–4°, 4–6°, 6–8°, 8–10°, 10–12°, 12–15° and 15–180° for the three elongation stages. It was seen that there is no obvious difference between length fractions for the three tension stages. This result is

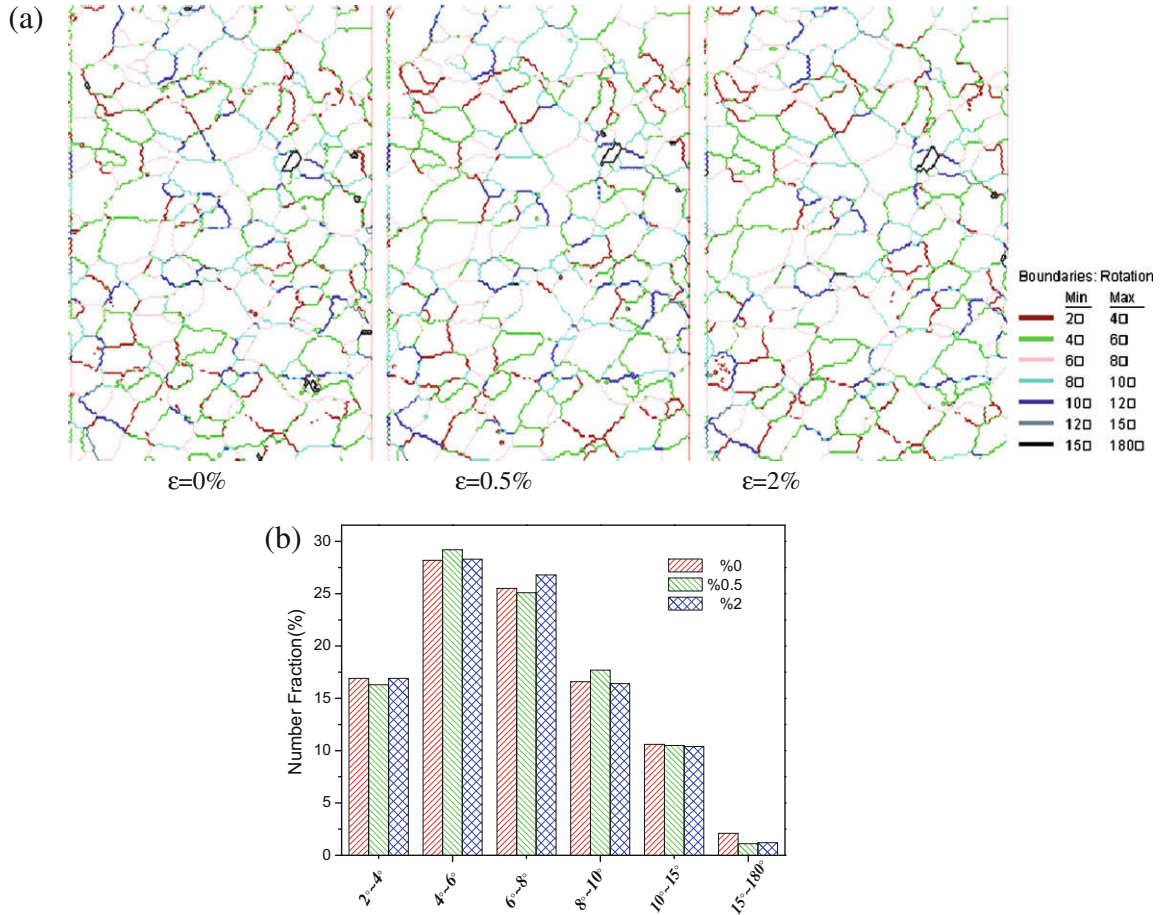


Fig. 7. (a) Grain boundary mappings and (b) grain boundary misorientation distributions of the outer Ni5W layers for various strain states.

also in good agreement with the grain boundary stability in the tensile processing, which is supposed to be favorable

for the epitaxial deposition of further buffer layers and YBCO films on this composite substrate.

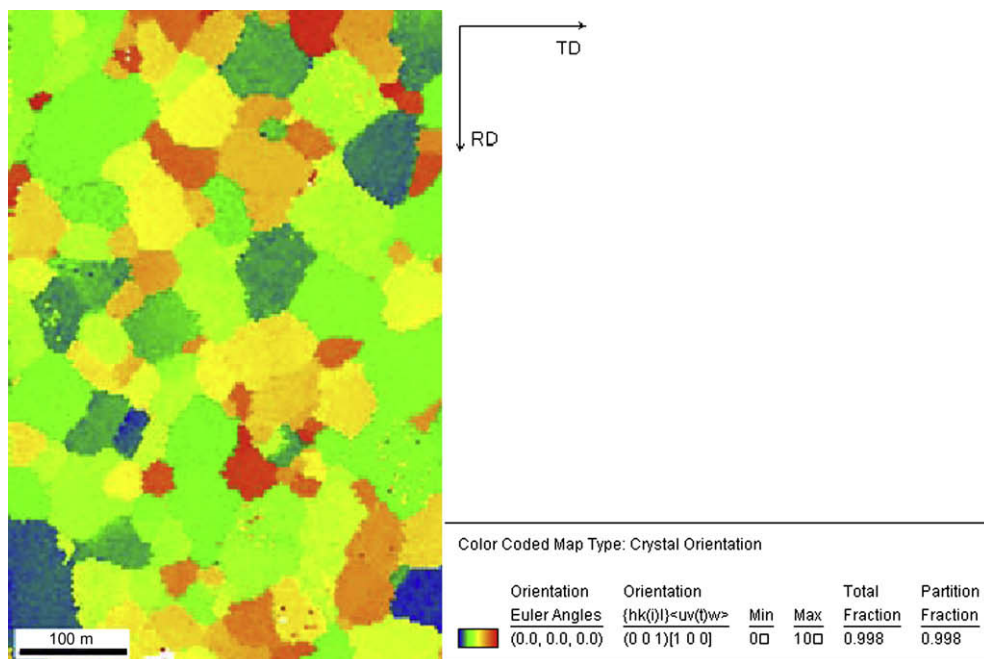


Fig. 8. EBSD image at Ni5W surface of the composite tape after severe annealing treatment.

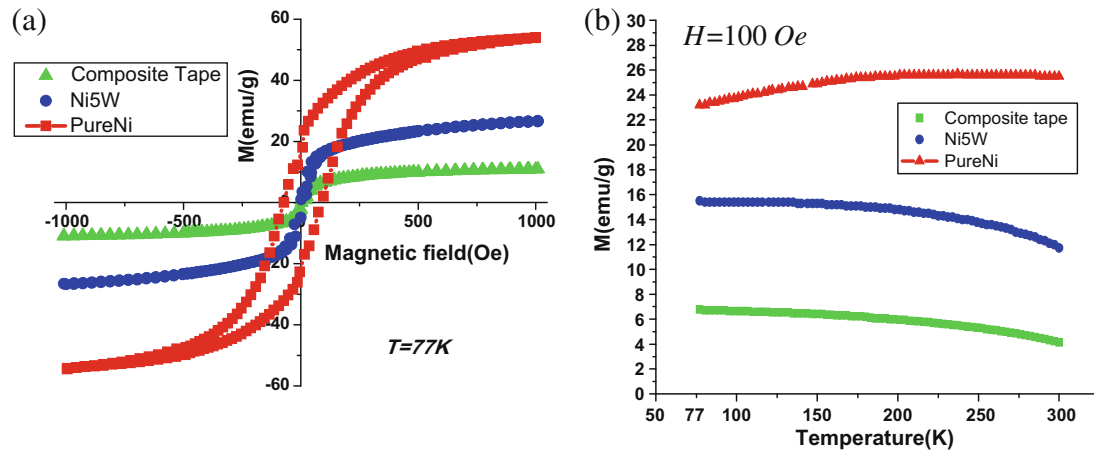


Fig. 9. (a) Magnetization loops at 77 K for pure Ni, Ni5W and Ni5W/Ni12W/Ni5W composite tapes and (b) mass magnetization as a function of temperature in pure Ni, Ni5W and Ni5W/Ni12W/Ni5W composite tapes.

3.5. Stability of the cube texture for the composite tapes at high-temperature

In order to investigate the texture stability of the composite tape in practical use such as epitaxial deposition of both buffer and YBCO layers, the as-obtained composite tapes have been studied at high-temperature up to 1250 °C, which is higher than the practical temperature for superconducting tape processing. Fig. 8 shows the EBSD mapping of the composite tape, which has been submitted to a high-temperature treatment at 1250 °C for 180 min. It was found that the cubic grain proportion with a misorientation angle of 10° is as high as 99.8%, indicating that a sharp cubic texture is still maintained at the Ni5W surface layer of the as-produced composite tape after carrying out an additional annealing. Due to the higher annealing temperature and longer annealing time than for the standard annealing procedure (1150 °C for 60 min), the grain sizes in the reannealed composite tape are slightly larger than that of the tape before reannealing. Fortunately, in spite of the longer annealing time, the abnormal growth of grains was not observed, which is possibly due to the diffusion of the W towards the outer layer, which thus suppresses the abnormal growth tendency. Consequently, the sharp cube texture at the Ni5W surface of the composite tape was successfully retained after submitting the tape to a tensile test and processing it again at high-temperature, demonstrating the stability of the composite substrate under a practical stress and high-temperature conditions.

3.6. Magnetization of the composite tapes

With respect to the practical use of coated conductors, the magnetic losses should be minimized in order to diminish energy losses in alternating current (AC) applications. Fig. 9a shows the $M-H$ hysteresis loops at 77 K (the operating temperature of coated conductors) for pure Ni, Ni-5% W (the same composition as the outer layer of our composite tape) and the composite tape (after recryst-

allization). It can be seen that the hysteresis losses for the composite substrate are strongly decreased in comparison with those of the pure Ni and the Ni5W substrates. Its saturation magnetization is reduced by approximately 80% and 40% in comparison with that of pure Ni and Ni5W substrate, respectively. The temperature dependence of mass magnetization $M(T)$ of the composite tape, together with the data for the Ni and Ni5W substrates measured in a magnetic field of 100 Oe applied parallel to the tape plane, is shown in Fig. 9b. The magnetization of the as-fabricated composite substrate is again greatly decreased. This result shows that the use of a Ni12W core for textured Ni5W/Ni12W/Ni5W composite tape considerably reduces the ferromagnetism while increasing the overall mechanical strength.

3.7. LZO buffer layer on Ni5W/Ni12W/Ni5W composite substrate

In order to prevent the diffusion of the substrate material (Ni) into the HTS (YBCO) film during the deposition,

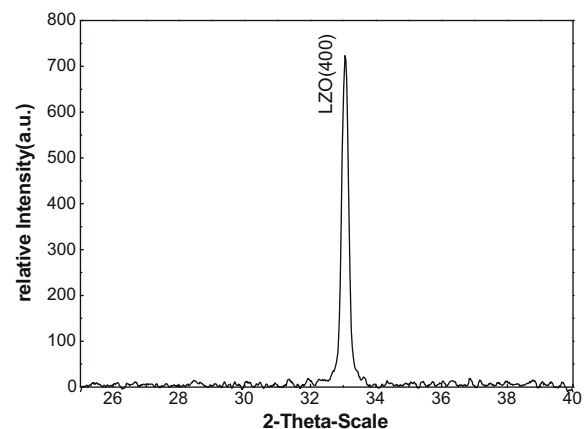


Fig. 10. XRD pattern of the LZO buffer layer deposited on Ni5W/Ni12W/Ni5W composite tape.

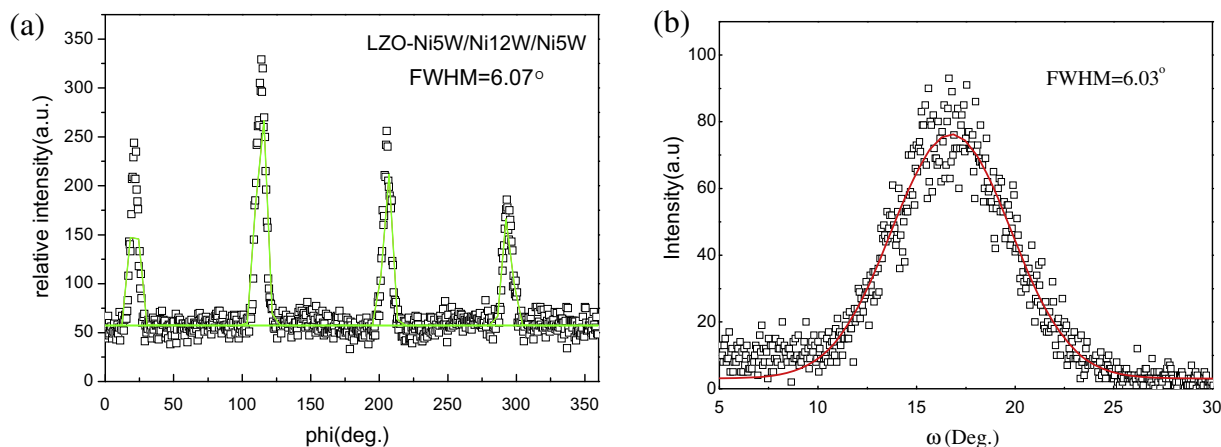


Fig. 11. (a) (2 2 2) ϕ -scan and (b) (4 0 0) rocking curve of the LZO buffer layer (the solid lines in the ϕ -scan and ω -scan are Gaussian fits to the data points).

while transferring the texture of the substrate to the conducting film, a thin (~ 100 nm) and biaxially textured LZO buffer layer was epitaxially deposited on the composite substrate by the MOD method before deposition of the YBCO film. The LZO precursor layer was annealed at 1150°C for 15 min. Conventional XRD was performed to analyze the phase in the as-deposited LZO buffer layer. Fig. 10 shows the XRD pattern of the LZO buffer layer on the Ni5W/Ni12W/Ni5W composite tape. There is only one LZO (4 0 0) ($2\theta = 33.3^\circ$) peak, indicating that the film had a well (0 0 1) oriented grain growth. The ϕ -scan and rocking curve (shown in Fig. 11) were used to evaluate the in-plane and out-of-plane texture of the samples annealed at 1150°C . In spite of the large lattice mismatch (8%) between the substrate and LZO, the FWHM values of the (2 2 2) ϕ -scan and the (4 0 0) rocking curve are 6.07° and 6.03° , respectively, indicating a sharp cube texture in the obtained LZO layer.

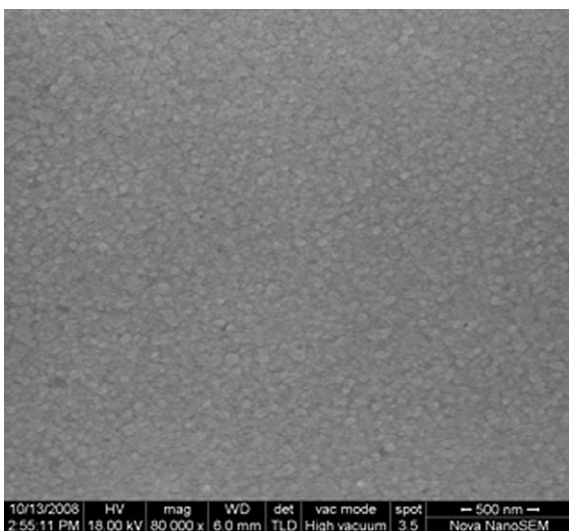


Fig. 12. SEM micrograph of the LZO buffer layer on the composite substrate.

In view of further deposition of other buffer and conducting layers, the surface condition of the as-fabricated LZO layer was also measured because defects such as microcracks and holes can significantly influence the quality of the further layers. Fig. 12 shows the micrograph of the LZO surface. It was observed that the LZO layer uniformly covers the substrate without any cracks or holes. Atomic force microscopy investigation of surface structure shows that the surface RMS roughness is about 6.52 nm in an area of $5\ \mu\text{m} \times 5\ \mu\text{m}$. The quality of the texture and the surface state of the LZO layer are therefore suitable for further deposition of other buffers or YBCO layer.

4. Conclusions

We have fabricated a Ni5W/Ni12W/Ni5W composite tape of $75\ \mu\text{m}$ thickness with the properties required for functional use as a substrate for coated conductor tapes. A particular three-layer technique was used, with textured Ni5W as the two outer layers and strong Ni12W as the core layer. These three layers are bonded by means of elemental diffusion. The diffusion layer formed between the outer layers and the core layer in the as-rolled composite tape becomes broader when the tapes were annealed at higher temperature, resulting from the W element migration from the core layer to the outer layers during recrystallization. The results show that the top Ni5W layer in the composite tape presents a sharp and pure (0 0 1) $\langle 100 \rangle$ cube texture, i.e. the most appropriate texture for high-quality YBCO-coated conductor tapes. The EBSD analysis performed in situ on both microtexture and grain boundaries of the Ni5W layer during tensile test of the composite tape shows that the volume fraction of the cubic grains and the relative length of grain boundaries with low misorientation angles are as high as 98% and 87%, respectively, for elongations of 2%, thus indicating that the cube texture and grain boundaries have a good stability under tensile conditions. Moreover, when applying an additional annealing treatment at 1250°C for 180 min, the Ni5W surface layer of

the composite tape still maintains a sharp cube texture. These results are significant and demonstrate the stability of the composite substrate under practical stress and high-temperature conditions. The composite tapes have markedly enhanced mechanical properties and lower magnetization with respect to both pure Ni and single Ni₅W layer substrates. A textured LZO buffer layer of high-quality has been deposited on this composite substrate. It is strongly believed that this composite tape is a promising and competitive candidate as a low-cost substrate with high and stable quality of cube texture and mechanical properties for large-scale coated conductor production in the near future.

Acknowledgments

This work was financially supported by National Basic Research Program 973 of China (2006CB601005), National Natural Science Foundation of China (50771003), National 863 Project of China (2007AA03Z242) and Beijing Municipal Natural Science Foundation (2092006).

References

- [1] Norton DP, Goyal A, Budai JD, Christen DK, Kroeger DM, Specht ED, et al. *Science* 1996;755:274.
- [2] Goyal A, Norton DP, Budai JD, Paranthaman M, Specht ED, Kroeger DM, et al. *Appl Phys Lett* 1996;69:1795–7.
- [3] Goyal A, Norton DP, Kroeger DM, Christen DK, Paranthaman M, Specht ED, et al. *J Mater Res* 1997;12:2924–40.
- [4] Matsumoto K, Kim SB, Wen JG, Hirabayashi I, Watanabe T, Uno N, et al. *IEEE Trans Appl Supercond* 1999;9(2):1539–42.
- [5] Cantoni C, Christen DK, Feenstra R, Goyal A, Ownby GW, Zehner DM. *Appl Phys Lett* 2000;79:3077–9.
- [6] Goyal A et al. *Physica C* 2002;382:251.
- [7] Eickemeyer J, Selbmann D, Opitz R, De Boer B, Holzapfel B, Schultz L, et al. *Supercond Sci Technol* 2001;14:152–9.
- [8] Zhang W et al. *Physica C* 2007;463–465:505.
- [9] <<http://www.evico.cc>>.
- [10] <<http://www.kisware.gr>>.
- [11] Subramanya Sarma V, Eickemeyer J, Schultz L, Holzapfel B. *Scr Mater* 2004;50:953.
- [12] Subramanya Sarma V, Eickemeyer J, Mickel C, Schultz L, Holzapfel B. *Mater Sci Eng A* 2004;380:30–3.
- [13] Goyal A. US Patent Nos. 6, 180, 570; 2001.
- [14] Goyal A. US Patent Nos. 6, 375, 768; 2002.
- [15] Watanabe T, Ohashi Y, Ozaki M, Yamamoto K, Maeda T, Wada K, et al. HTS conductors, processing and applications. In: The 2002 international workshop on superconductivity (the 5th joint ISTEC/MRS workshop), Honolulu, HI; 2001. p. 21–4.
- [16] Suo HongLi, Zhao Yue, Liu Min, He Dong, Zhang YingXiao, Zhou MeiLing. *IEEE Trans Appl Supercond* 2007;17(2):3420–3.
- [17] Zhao Yue, Suo Hongli, Liu Min, He Dong, Zhang YingXiao, Ma Lin, et al. *Acta Mater* 2007;55:2609–14.
- [18] Suo Hongli, Zhao Yue, Liu Min, Zhang YingXiao, He Dong, Ma Lin, et al. *Acta Mater* 2008;56:23–30.
- [19] Eickemeyer J, Selbmann D, Opitz R, de Boer B, Holzapfel B, Schultz L, et al. *Supercond Sci Technol* 2001;14:152.
- [20] Goyal A, Norton DP, Kroeger DM, Christen DK, Paranthaman M, Specht ED. *J Mater Res* 1997;12:2924.
- [21] Goyal A, Paranthaman M, Schoop U. *MRS Bull* 2004;29:552–61.